

# Investigation of Signal Processing Algorithms for an Embedded Microcontroller-Based Wearable Pulse Oximeter

W. S. Johnston, and Y. Mendelson\*, *Member, IEEE*

**Abstract**—Despite steady progress in the miniaturization of pulse oximeters over the years, significant challenges remain since advanced signal processing must be implemented efficiently in real-time by a relatively small size wearable device. The goal of this study was to investigate several potential digital signal processing algorithms for computing arterial oxygen saturation (SpO<sub>2</sub>) and heart rate (HR) in a battery-operated wearable reflectance pulse oximeter that is being developed in our laboratory for use by medics and first responders in the field. We found that a differential measurement approach, combined with a low-pass filter (LPF), yielded the most suitable signal processing technique for estimating SpO<sub>2</sub>, while a signal derivative approach produced the most accurate HR measurements.

## I. INTRODUCTION

Steady advances in wearable physiological monitoring, such as hardware miniaturization and RF communication, are leading to the development of new wireless technologies that have broad and important implications for various medical applications [1]-[2]. For example, the emerging development of compact and light-weight wearable devices could facilitate remote noninvasive monitoring of vital signs from soldiers during training exercises and combat [3]. Small size wearable devices can also be useful for mission specialists or emergency first-responders operating in harsh and hazardous environments. The primary goal of this technology would be to keep track of an injured person's vital signs via a short-range wirelessly linked personal area network, thus readily enabling telemetry of physiological information to field medics, command units, and secured medical facilities.

Presently, continuous physiological monitoring from mobile soldiers during combat using commercially available pulse oximeters is unsuitable. The main problems involve cumbersome devices, sensor attachment, and unwieldy wires. Additionally, sensor attachment to a subject's finger,

a common practice in many clinical applications, interferes with normal physical activity and measurements would be susceptible to motion artifacts. Hence, there is a need to develop a more robust pulse oximeter that is suitable for noninvasive monitoring of arterial oxygen saturation (SpO<sub>2</sub>) and heart rate (HR) from mobile persons without restraining normal physical activities.

Although most commercial pulse oximeters employ complex signal processing to improve measurement accuracy and reduce the effects of motion artifacts, these devices have limited utility as wearable devices for extended field applications mainly due to size and power constraints. Despite steady progress in the miniaturization of pulse oximeters, significant challenges remain because advanced signal processing must be implemented efficiently in real-time by a relatively small size microcontroller. Therefore, the goal of this study was to investigate several potential digital signal processing algorithms for computing SpO<sub>2</sub> and HR in a wearable reflectance pulse oximeter that is being developed in our laboratory [4]-[6].

## II. METHODOLOGY

### A. SpO<sub>2</sub> Experiments

*Experimental Setup:* A transmission-type Nonin Xpod<sup>®</sup> pulse oximeter was used to acquire reference SpO<sub>2</sub> readings from a subject's index finger. Reflected red (R) and infrared (IR) photoplethysmograms (PPG) were acquired from an optical sensor that was secured to the subject's forehead using an elastic headband. Separate R and IR PPG were obtained from a custom photoplethysmographic signal processing unit (PSPU) at a rate of 100 s/s. Figure 1 shows the experimental setup.

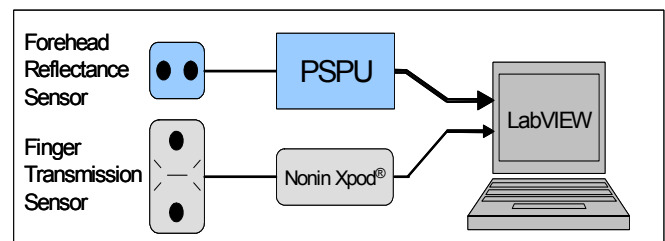


Fig 1. Experimental Setup for SpO<sub>2</sub> and PPG Acquisitions.

*In Vivo Experiments:* Data were acquired from three healthy male volunteers, ages 24–25 while the subjects rested comfortably in a chair. Following 20s of baseline recording, subjects were instructed to hold their breath to induce a hypoxic episode and resume normal breathing.

Manuscript received April 3, 2006. This work is supported by the U.S. Army Medical Research and Materiel Command under Contract No. DAMD17-03-2-0006. The views, opinions and/or findings are those of the author and should not be construed as an official Department of the Army position, policy, or decision, unless so designated by other documentation.

W. S. Johnston is a M.Sc. student in the Department of Biomedical Engineering, Worcester Polytechnic Institute, Worcester, MA 01609 USA (phone: 508-831-5891; fax: 508-831-5541; e-mail: johnston@wpi.edu).

\*Corresponding author – Y. Mendelson is a Professor in the Department of Biomedical Engineering, Worcester Polytechnic Institute, Worcester, MA 01609 USA (e-mail: ym@wpi.edu).

## B. HR Experiments

*Experimental Setup:* An infrared reflectance-type sensor was used to record PPG waveforms from the forehead. The sensor was secured in place using an elastic headband. Three disposable ECG electrodes were used to record simultaneously a standard *lead I* ECG waveform to establish a HR reference. The analog signals from each sensor were amplified by a set of PPG and ECG amplifiers (BIOPAC Systems) and then acquired in real-time by a PC at a rate of 200s/s. Figure 2 shows the corresponding experimental setup.

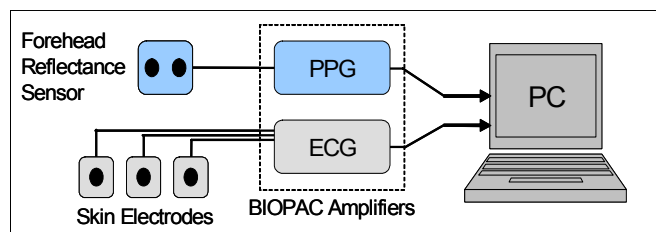


Fig. 2. Experimental Setup for HR Recording.

*In Vivo Experiments:* Baseline HR were acquired from three healthy male volunteers, ages 23 – 25 while the subjects rested comfortably in a chair. Following a one-minute baseline recording, subjects were asked to jog in place to induce tachycardia.

## C. SpO<sub>2</sub> Processing Algorithms

Several signal processing algorithms were investigated to determine the DC and AC components of each PPG. Analysis of the R and IR PPG signals to compute SpO<sub>2</sub> was based on an empirical calibration relationship given by

$$R = (R / IR) = \frac{\left( \frac{AC_R}{DC_R} \right)}{\left( \frac{AC_{IR}}{DC_{IR}} \right)}$$

where the time-variant (AC) and time-invariant (DC) components of the respective R and IR PPG waveforms were calculated to form a normalized “ratio-of-ratios” variable, denoted by  $R$ .

*DC Measurements:* Three different processing methods were employed to measure the DC value of each PPG. The first method involved a three-second moving average of the most recent samples. The second method utilized a 5<sup>th</sup> order,  $f_c=0.1$ Hz, IIR Butterworth LPF. The third analysis used the minimum value in a three-second window of the most recent PPG samples.

*AC Measurements:* Five different processing methods were employed to determine the AC amplitudes of the PPG signals. Four of the AC measurement methods were paired with each of the three independent DC measurement techniques, yielding a set of 13 unique processing methods.

The first approach used a three-second time average of local PPG derivatives. The second signal processing approach first utilized signal derivatives to identify

individual PPG pulses and subsequently the amplitude difference between the peak and nadir of each pulse was determined. The third technique used the most recent three-second AC/DC normalized derivatives of the PPG to calculate a regression slope, where the values corresponding to the R PPG signals were regressed against the normalized derivatives of the corresponding IR PPG signals. The regression slope was then converted to an angle that was used in place of an  $R$  value. In the fourth approach, we used the difference between the maximum and minimum values of the PPG waveform in a three-second window spanning the most recent data points. Finally, we also investigated an optimized spectral analysis approach by processing every 5<sup>th</sup> data point in the PPG using a 64-point FFT. This resulted in a transform that assessed 4.3s of a PPG signal while still providing information over the full span of the cardiac frequency range (0.5 – 5Hz). The amplitude of the highest peak in the cardiac frequency range was used as the AC component of the PPG.

## D. HR Processing Algorithms

Three signal processing algorithms were investigated as potential methods for measuring HR based on the IR PPG. The first approach was based on a varying-width adaptive window to locate individual pulse peaks in the PPG. The sliding window scanned the PPG waveform using one data point increments. After each step, the maximum value in the window was located. If the maximum value detected was in the center of the window, the data point was marked as a peak. To account for instantaneous variations in HR, the width of the processing window was adjusted each time a peak was located. The new window width was set to half the length of the previous beat-to-beat interval. This reduced the chances of identifying two peaks inside the window while maintaining a reduced sensitivity to noise and minor signal irregularities. Each beat-to-beat interval was first converted to an instantaneous heart rate (IHR) value. All IHR values from a one-minute PPG segment were subsequently averaged to produce a single HR measurement.

In the second analysis approach, we used a two-point derivative of the PPG to identify individual pulse peaks. These derivatives were assessed one data point at a time. Each point was compared to a predetermined threshold value. When the data point exceeded this threshold, it was used to indicate the occurrence of the systolic slope in the PPG. Subsequently, the following zero-crossing in the derivative was marked as a peak. To account for variations in slopes due to changes in HR and pulse shape, the threshold was adjusted every time a new peak was located. This procedure minimized noise and minor signal irregularities from being falsely identified, while simultaneously also reducing the chances of missing a systolic phase due to a shallow slope.

The third algorithm to compute HR was based on spectral analysis of the PPG. Accordingly, FFT were computed based on one-minute PPG segments, and the largest peak in the cardiac frequency range between 0.5–5Hz in each FFT were used to obtain an IHR measurement.

### III. RESULTS

TABLE I  
SpO<sub>2</sub> PROCESSING ALGORITHMS

AC Values	DC Values	R <sup>2</sup> Value	Bias (%)	SEE (%)
Differentials	Moving Average	0.96	-0.0007	0.84
	LPF	0.97	0.0001	0.82
	Window Minimum	0.96	-0.0028	0.91
Pulse Amplitudes	Moving Average	0.97	0.0037	0.82
	LPF	0.97	0.0022	0.91
	Window Minimum	0.97	-0.0016	0.81
Regression Analysis	Moving Average	0.92	0.0019	1.37
	LPF	0.96	-0.0008	1.11
	Window Minimum	0.95	0.0001	0.96
Window Analysis	Moving Average	0.90	-0.0021	1.38
	LPF	0.90	-0.0030	1.41
	Window Minimum	0.89	0.0002	1.44
Spectral Analysis	Spectral Analysis	0.96	-0.0040	0.84

TABLE II  
HR PROCESSING ALGORITHMS

Processing Methods	R <sup>2</sup> Value	Bias (bpm)	SEE (bpm)
Moving Window	0.64	6.62	15.48
Signal Derivative	0.99	0.43	1.27
Spectral Analysis	0.90	-2.45	4.98

### IV. DISCUSSION

Compared with small wearable pulse oximeters, clinical units have unlimited power resources. These additional resources allow the manufacturers to employ advanced digital signal processing techniques that provide a high degree of accuracy which is important for routine clinical applications. For field applications, however, it is important to consider additional design constraints in order to optimize the size and power consumption of a wearable physiological monitoring device. Furthermore, these design constraints must be met efficiently without significantly degrading the overall performance characteristics of the wearable device.

In designing miniature, robust, and power efficient wearable physiological devices for field applications, especially for use by soldiers during combat, it must be kept in mind that processing capabilities must be further optimized in order to conserve power consumption which might be supplied by a small coin-cell battery. Therefore, for field triage applications, the signal processing methods

employed must be simplified to minimize processing requirements, and yet effective enough to provide accurate physiological information.

Among the different methods assessed to calculate SpO<sub>2</sub> in Table I, we found that the three processing algorithms employed to measure the DC component of each PPG produced minimal SpO<sub>2</sub> differences when paired with the same AC measurement approach. Of the five time and frequency domain algorithms we investigated as potential candidates for processing the AC components of each PPG, we found that the differential measurements produced the best overall results. Considering the different combinations investigated in this study, we determined that the most accurate method for calculating SpO<sub>2</sub> was based on the differential measurement approach and a LPF algorithm, which were used to obtain the AC and DC components, respectively. The regression analysis resulting from the data that were analyzed by the preferred algorithms (shaded in Table I) is shown in Fig. 3.

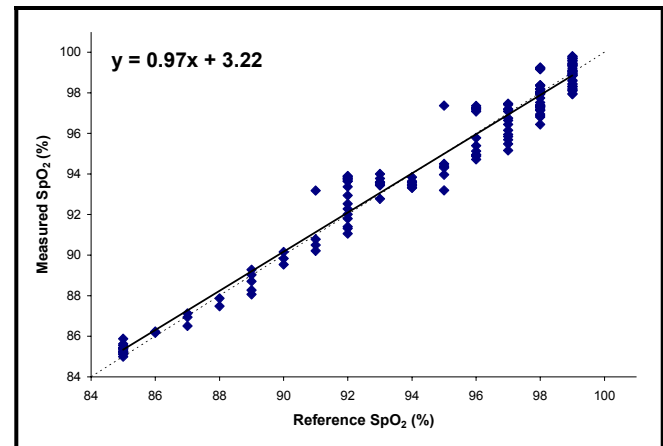


Fig. 3. Regression Analysis using the Differentials-LPF Algorithm for SpO<sub>2</sub> Calculations with Resulting Regression Line (—) and Line of Identity (---).

Among the three potential signal processing algorithms that were investigated for the purpose of computing HR from a PPG waveform, we found that the time series analysis of the PPG derivative produced superior accuracy with respect to all the assessment variables. As shown in Table II, the signal derivative approach performed significantly better compared to the other two algorithms that we have investigated in this study. Fig. 4 shows the regression analysis corresponding to the data that were analyzed by the signal derivative algorithm (shaded area in Table II).

Assessment of measurement accuracy was of primary concern during the selection of SpO<sub>2</sub> and HR processing methods. Following the selection of the two most appropriate algorithms, the software resources required to implement the methods were examined. Table III summarizes the memory and instruction cycles needed to execute each method from within the dsPIC30F6014 microcontroller environment.

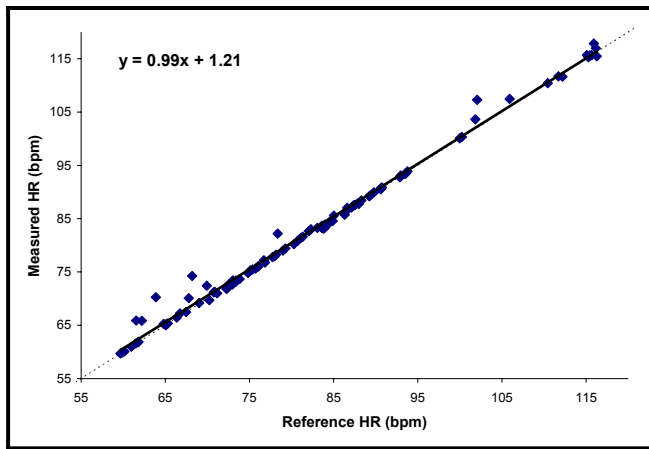


Fig. 4. Regression Analysis using the Signal Derivative Algorithm for HR Calculations with Resulting Regression Line (—) and Line of Identity (---).

TABLE III  
SUMMARY OF REQUIRED SOFTWARE RESOURCES

Measurement	Program Memory (bytes)	Data Memory (bytes)	Processing Cycles	
			Single Execution	Per Second
SpO <sub>2</sub>	2601	982	17,376	17,376
HR	678	48	1818	136,350

Physical size and power consumption are critical features in wearable medical devices since device transparency to a user and extended battery life directly influence effectiveness in field-based applications. To provide flexibility during development, the processing core of the prototype device was the dsPIC30F6014 microcontroller that contained 144K bytes of program memory and 8192 bytes of data memory. Due to the low memory requirements of the selected processing methods, the possibility exists to implement a more efficient processing core in the hardware portion of the design, potentially resulting in reduced cost, weight, physical size, and power consumption.

We also performed a preliminary assessment of processing speed. Based on the dsPIC30F6014 microprocessor and the cycle counts noted in Table III, the microcontroller dedicated 2% of every second to processing new measurements. However, in a worst-case scenario, up to 20% of a single sample interval (i.e., 13.3 ms) could be dedicated to process new measurements. As demonstrated by these assessments, timing requirements are much more dynamic in real-time signal processing than simple memory allocation. Therefore, time budgeting should be carefully evaluated before the software is implemented in an alternative microcontroller with potentially limited processing resources.

## V. CONCLUSIONS

In this study, we investigated several potential signal processing algorithms that are suitable for measuring SpO<sub>2</sub> and HR by a battery-operated, wearable pulse oximeter. The

study revealed that a differential measurement approach, combined with a LPF algorithm, yielded the most suitable signal processing technique for real-time estimation of SpO<sub>2</sub>, while a signal derivative approach produced the most accurate HR measurements. Assessments of software resources required to implement the processing methods showed that reduced memory allocation could allow the use of a smaller and more power efficient processor, but also highlighted the importance of evaluating software timing characteristics when altering key components of the design such as the core microcontroller.

## ACKNOWLEDGMENT

The authors would like to acknowledge the financial support provided by the U.S. Army Medical Research and Material Command referenced.

## REFERENCES

- [1] G. S. F. Ling, B. K. Day, P. Rhee, and J. M. Ecklund, "In search of technological solutions to battlefield management of combat casualties," *SPIE Conference on Battlefield Biomedical Technologies*, SPIE vol. 3712, Apr. 1999.
- [2] D. Malan, T. Fulford-Jones, M. Welsh, and S. Moulton, "CodeBlue: An ad-hoc sensor network infrastructure for emergency medical care," *International Workshop on Wearable and Implantable Body Sensor Networks*, 2004.
- [3] Y. Mendelson and V. Floroff, "A PDA based *ad-hoc* mobile wireless pulse oximeter," *Proc. IASTED International Conference Telehealth 2005*, Banff, Canada, 2005.
- [4] Y. Mendelson and C. J. Pujary, "Minimization of LED power consumption in the design of a wearable pulse oximeter," *IASTED International Conference BioMED 2003*, Salzburg, Austria, 2003.
- [5] Y. Mendelson and C. J. Pujary, "Measurement site and photodetector size considerations in optimizing power consumption of a wearable reflectance pulse oximeter," *Proc. of the 25<sup>th</sup> Annual International IEEE/EMBS Conference*, Cancun, Mexico, 2003.
- [6] P. Branche and Y. Mendelson, "Signal quality and power consumption of a new prototype reflectance pulse oximeter sensor," *Proc. of the 31<sup>th</sup> Annual Northeast Bioengineering Conference*, Hoboken, NJ, 2005.